

Quadrupole Orders on the fcc Lattice

Hirokazu Tsunetsugu¹, Takayuki Ishitobi² and Kazumasa Hattori²

¹ *The Institute for Solid State Physics, The University of Tokyo, Kashiwanoha 5-1-5, Chiba 277-8581, Japan*

² *Department of Physics, Tokyo Metropolitan University, Hachioji, Tokyo 192-0397, Japan*

We theoretically study electric quadrupole orders in f-electron systems on the fcc lattice. Quadrupole degrees of freedom O_{20} and O_{22} originate in the non-Kramers doublet ground state Γ_3 of ion with f^2 electron configuration. For discussing quadrupole orders, we use a minimal model with isotropic (J) and anisotropic (K) nearest-neighbor interactions, and determine the phase diagram using a four-site mean-field approximation at zero and finite temperatures. Quadrupoles couple the Γ_3 doublet to the singlet excited state Γ_1 , and its effects on canting antiferro orders are examined in detail. We found that this coupling leads to a rich phase diagram including two- and four-sublattice antiferro phases, and that two phases show a partial order of quadrupoles at finite temperatures.

Several years ago, the authors studied antiferro quadrupole orders in Pr 1-2-20 compounds,¹⁻³⁾ where Pr ions form a diamond sublattice. Pr 1-2-20 systems show various exotic phenomena such as non Fermi liquids, superconductivity, and multipolar phase transitions.⁴⁾ Each Pr^{3+} ion has two f -electrons and its ground state is a non-Kramers doublet Γ_3 in cubic environment. In Γ_3 doublet, electric quadrupole has two active components O_{20} and O_{22} , and they form a two-dimensional basis $\mathbf{Q}=(Q_u, Q_v)$ of E irreducible representation of the cubic point group. They show a long-range order at low temperatures into *e.g.*, ferro phase for $\text{PrTi}_2\text{Al}_{20}$,⁵⁻⁷⁾ antiferro phase for $\text{PrIr}_2\text{Zn}_{20}$,^{8,9)} and density-wave phase for PrPb_3 .^{10,11)}

From a theoretical view point, one expects many similarities between these quadrupole systems and easy-plane magnets since both groups have a two-component order parameter, but two points sharply distinguish between their order parameters. One is about the time-reversal symmetry: \mathbf{Q} has an even parity while magnetization's is odd. The other is their transformation rule upon point-group symmetry operations, since \mathbf{Q} is a second-rank tensor while magnetization is an axial vector. Therefore, despite quite many theoretical studies on planar magnets, new studies are necessary for clarifying characteristics of quadrupole orders.¹²⁾

Recently, Kusanose *et al.* have studied another compound PrMgNi_4 and discussed an antiferro quadrupole order.^{13,14)} This material has Pr ions on a fcc sublattice, and we will show that this difference in lattice structure has important implications for quadrupole orders. This is due to different effective quadrupole interactions between the two lattice structures. In the diamond lattice, Pr-Pr nearest-neighbor bonds point to [111] and equivalent directions, and this limits interactions to isotropic ones $J\mathbf{Q}(\mathbf{r}) \cdot \mathbf{Q}(\mathbf{r}')$.¹⁾ This isotropic interaction has been used for effective Hamiltonians modeling the Pr 1-2-20 system.^{1,2,15-17)}

We have performed symmetry analysis and found that quadrupole interactions on the fcc lattice generally have anisotropic terms in addition to isotropic ones. Each site is surrounded by twelve nearest neighbors separated by $\delta_{1,2} = (0, 1, \pm 1)/2$, $\delta_{3,4} = (\pm 1, 0, 1)/2$, $\delta_{5,6} = (1, \pm 1, 0)/2$, and their counterparts $-\delta$'s as shown in Fig. 1(a). The minimal model

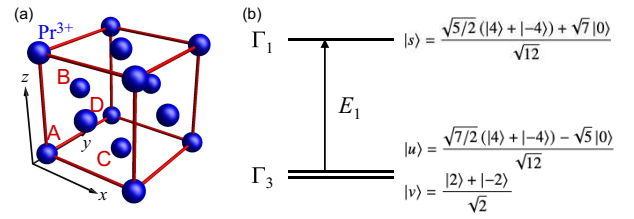


Fig. 1. (color online). (a) fcc lattice of Pr ions and its four sublattices labeled by A-D. $\overline{AB}=\delta_1$, $\overline{AC}=\delta_5$, and $\overline{AD}=\delta_3$. (b) Non-Kramers ground-state doublet Γ_3 and singlet excited state Γ_1 of Pr^{3+} ion. $|m\rangle$ is the eigenstate $J_z|m\rangle = m|m\rangle$ in the $J=4$ multiplet.

of quadrupole interactions in Γ_3 levels reads as

$$H_Q = \sum_{\mathbf{r}} \sum_{j=1}^6 \mathbf{Q}(\mathbf{r}) \cdot [J1 + Kg(\delta_j)] \mathbf{Q}(\mathbf{r} + \delta_j), \quad (1)$$

where K is the anisotropic coupling constant and 1 is the two-dimensional identity matrix. Another parametrization $(J, K) = \bar{J}(\cos \xi, \sin \xi)$ will be also used in this paper. Here, the \mathbf{r} -sum is taken over all the sites in the fcc lattice and \mathbf{Q} operates in the Γ_3 doublet as $Q_u = |u\rangle\langle u| - |v\rangle\langle v|$ and $Q_v = -|u\rangle\langle v| - |v\rangle\langle u|$ in terms of the basis states shown in Fig. 1(b). The anisotropy factor is defined as

$$g(\delta) = \cos \zeta(\delta) \hat{\sigma}_3 - \sin \zeta(\delta) \hat{\sigma}_1, \quad (2)$$

where $\hat{\sigma}_{1,3}$ are Pauli matrices, and $(\cos \zeta(\delta), \sin \zeta(\delta)) \propto (2z^2 - x^2 - y^2, \sqrt{3}(x^2 - y^2))$ for $\delta = (x, y, z)$. Note that $\zeta(\pm\delta_{3,4}) = -\zeta(\pm\delta_{1,2}) = \pi/3$.

Let us first find a classical ground state of this Hamiltonian. Performing Fourier transformation, the Hamiltonian is represented as $H_Q = \sum_{\mathbf{k}} \mathbf{Q}_{\mathbf{k}} \cdot [J\gamma_0(\mathbf{k}) + K\boldsymbol{\gamma}(\mathbf{k})] \mathbf{Q}_{-\mathbf{k}}$ with the coefficients $\gamma_0(\mathbf{k}) = 2(c_x c_y + c_y c_z + c_z c_x)$, $\boldsymbol{\gamma}(\mathbf{k}) = [(c_x + c_y)c_z - 2c_x c_y] \hat{\sigma}_3 - \sqrt{3}(c_x - c_y)c_z \hat{\sigma}_1$, where $c_a \equiv \cos(ka/2)$. This effective model was obtained with the special value $K=J$ by Kubo and Hotta¹⁸⁾ starting from a microscopic Hamiltonian. The special K value is due to a simple form of the used microscopic Hamiltonian, but various other types of super-exchange processes generate $K \neq J$.

A classical ground state is a spiral state with the wavevector \mathbf{k} where the coefficient matrix $J\gamma_0 + K\boldsymbol{\gamma}$ has the minimum

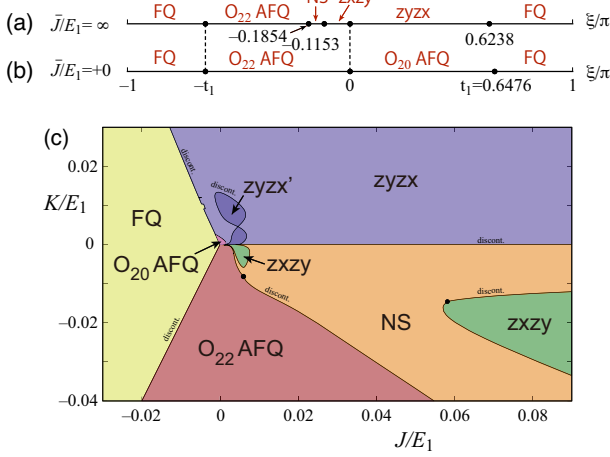


Fig. 2. (color online). Ground-state phase diagram determined by a 4-sublattice mean field theory. (a) Results in the limit $\bar{J}/E_1 = \infty$. (b) The opposite limit $\bar{J}/E_1 = +0$, and this corresponds to the model H_Q . t_1 is the point where $K = -2J > 0$. (c) Results in the J - K space. Black dots are tri-critical points separating continuous and discontinuous transitions. $zyzx'$ phase is a special case that $|\langle Q \rangle|$ is pinned to 1 in one sublattice.

eigenvalue. We can easily show that the ordering wavevector is $\mathbf{k}_X = (0, 0, 2\pi)$ when $|K| + 2J > 0$, and $\mathbf{k}_0 = (0, 0, 0)$ when $2J < |K| < -2J$. They correspond to antiferro quadrupole (AFQ) and ferro quadrupole (FQ) order, respectively. Judging from the corresponding eigenvector, the AFQ order parameter is $(-1)^{2z} \langle Q_u(\mathbf{r}) \rangle$ for $K > 0$ and $(-1)^{2z} \langle Q_v(\mathbf{r}) \rangle$ for $K < 0$, which are A-type antiferro order of O_{20} and O_{22} moments, respectively. Each AFQ phase has the degeneracy $6 = 3 \times 2$: the factor 3 comes from the equivalence of \mathbf{k}_X with $(2\pi, 0, 0)$ and $(0, 2\pi, 0)$, while the factor 2 relates to the exchange of \pm signs. Note that the use of a different \mathbf{k} also requires a mirror operation in (Q_u, Q_v) space,¹⁾ since both come from a same $\pi/2$ -rotation operation in \mathbf{r} -space. In the ferro phase, the K -term contribution vanishes and the quadrupole internal space is isotropic. Therefore, the direction of FQ moment is arbitrary, but we will show later that this isotropy is broken by the coupling to Γ_1 excited state. We have confirmed that the mean-field theory predicts the same ground-state phase diagram, and the result is shown in Fig. 2(b). We have also studied the related finite temperature phase transition using the standard mean field theory. The transition temperature is $T_c = 12|J|$ for FQ phase, while $T_c = 4J + 8|K|$ for AFQ phase irrespective of the sign of K . Phase transitions at finite temperatures are all second order except for bi-critical points $|K| = -2J$ and $T_b = 6|K|$.

The $K > 0$ and $K < 0$ parts of the phase diagram are related by a symmetry of the Hamiltonian (1) at both $T = 0$ and $T > 0$. The $\pi/4$ -rotation in Γ_3 Hilbert space transforms the operators as $Q \rightarrow i\hat{\sigma}_2 Q$. Operated by this transformation, the Hamiltonian remains invariant except for the sign change $K \rightarrow -K$, since $(i\hat{\sigma}_2)^\dagger \mathbf{g}(\mathbf{r})(i\hat{\sigma}_2) = -\mathbf{g}(\mathbf{r})$. This explains the symmetry in the phase diagram. We will see below that coupling to the Γ_1 excited state breaks this symmetry.

Now, let us study the effects of the singlet excited state Γ_1 , and denote its energy by E_1 . An important new feature is an induced Z_3 anisotropy in the internal Q space, and this modifies the ordered states. We have studied this issue for Pr 1-2-

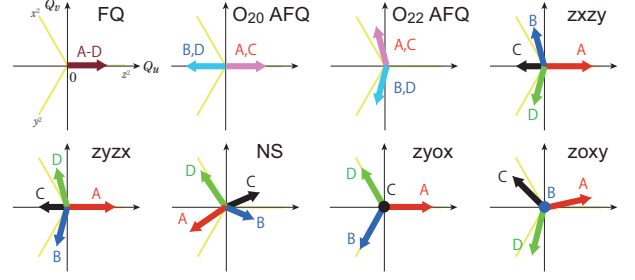


Fig. 3. Ordered phases of quadrupoles. Typical sublattice $\langle Q \rangle$ -configurations are shown, and color distinguishes different sublattices A-D. Yellow lines show Z_3 principle axes corresponding to the symmetries $3z^2 - r^2$, $3x^2 - r^2$, and $3y^2 - r^2$. Note moments in the zox phase are generally inclined from the Z_3 axes.

20 compounds, for which $K = 0$ and showed that a parasite FQ moment emerges in AFQ orders.¹⁾ Quadrupole operators connect Γ_3 doublet with Γ_1 singlet $|s\rangle$, and thus the Hamiltonian (1) should be modified as

$$H = E_1 \sum_{\mathbf{r}} |s(\mathbf{r})\rangle \langle s(\mathbf{r})| + H_Q [Q \rightarrow Q^{(\Gamma_3 + \Gamma_1)}], \quad (3)$$

$$Q_w^{(\Gamma_3 + \Gamma_1)} = Q_w + \alpha [|s\rangle \langle w| + \text{h.c.}], \quad \alpha \equiv \frac{\sqrt{35}}{2}, \quad (4)$$

for $w = u, v$.¹⁾ In the following, the quadrupole operators Q refer to those generalized $Q^{(\Gamma_3 + \Gamma_1)}$. It is clear that the new operators do not have the aforementioned symmetry upon $\pi/4$ -rotation in Γ_3 space.

As before, let us examine symmetry breaking in the ground state by the mean field theory. A crucial difference from the previous calculation is that now the response $\langle Q \rangle$ generally does not parallel its molecular field $\mathbf{h} = :h(\cos \eta, \sin \eta)$. When $h \ll E_1$, one can use the degenerate perturbation theory and calculate the response. Consider a single-site mean field Hamiltonian $H_{\text{mf}} = E_1 |s\rangle \langle s| - \mathbf{h} \cdot \mathbf{Q}$. Its ground state is $|\psi_0\rangle \approx \cos(\eta/2)|u\rangle - \sin(\eta/2)|v\rangle + (\alpha h/E_1) \cos(3\eta/2)|s\rangle$, and the response is immediately obtained

$$\begin{bmatrix} \langle Q_u \rangle \\ \langle Q_v \rangle \end{bmatrix} \approx \frac{\mathbf{h}}{h} + \chi_1 \mathbf{h} + \chi_1 h \begin{bmatrix} \cos 2\eta \\ -\sin 2\eta \end{bmatrix}, \quad \chi_1 \equiv \frac{\alpha^2}{E_1}. \quad (5)$$

The last term is not parallel to \mathbf{h} , unless $\eta = (\pi/3) \times (\text{integer})$. This manifests that the Q -space symmetry is reduced down to Z_3 , compared with the $O(2)$ symmetry in the mean field approximation of H_Q .

In the two-sublattice AFQ phase, the molecular fields of the A- and B-sublattices are related to the two order parameters as $\mathbf{h}^A = -4(J - K\hat{\sigma}_3)\langle Q^A \rangle - 4(2J + K\hat{\sigma}_3)\langle Q^B \rangle$, and Q^A and Q^B are exchanged for \mathbf{h}^B . The O_{20} AFQ phase has the solution $\langle Q^A \rangle \approx (1 + 35(J + 2K)/E_1, 0)$ with $\langle Q_u^B \rangle = (-1, 0)$ unchanged. The FQ phase's solution is $\langle Q \rangle \approx (1 + 210|J|/E_1, 0)$. Note that the order parameter angle points to one of the Z_3 axes, where $|\langle Q \rangle|/|h|$ is maximum. Calculation for the O_{22} AFQ phase is more elaborate. Since $\mathbf{h}^{A,B}$ and $\langle Q^{A,B} \rangle$ are not parallel, one needs to determine the tilting of the molecular field $\eta^{A,B} = \pm(\pi/2 + \delta\eta)$ self-consistently. The result is

$$\langle Q^A \rangle \approx \begin{bmatrix} \delta\eta \\ 1 \end{bmatrix} + 35 \frac{J + 2|K|}{E_1} \begin{bmatrix} -1 \\ 1 \end{bmatrix}, \quad \delta\eta = \frac{105J(J + 2|K|)}{2(2J + |K|)E_1}, \quad (6)$$

and $\langle Q^B \rangle = \hat{\sigma}_3 \langle Q^A \rangle$. Note that $\delta\eta$ diverges with approaching the boundary to the FQ phase.

When the Γ_1 level is not high, the perturbation theory breaks down, and we need numerical calculations to solve the mean field equations self-consistently. In the FQ phase ($2J < K < 2|J|$), the order parameter $\langle Q_u \rangle$ approaches continuously to the maximum limit $7/2$ as $|J|/E_1 \rightarrow \infty$. The coupling to Γ_1 level changes the AFQ orders drastically. It destabilizes the 2-sublattice structure such as simple O_{20} or O_{22} order, and 4-sublattice orders appear in a wide parameter range.

Let us first examine the limit of strong interactions $\bar{J}/E_1 \rightarrow \infty$. We have performed a mean-field analysis using four sublattices and found 5 phases as shown in Fig. 2 (a). Recall $(J, K) = \bar{J}(\cos \xi, \sin \xi)$. Compared to the weak interaction limit $\bar{J}/E_1 = +0$, the O_{20} phase is mainly replaced by the $zyzx$ phase, and a considerable part of the O_{22} phase is replaced by the $zxzy$ phase and the nonsymmetric (NS) 4-sublattice phase. Sublattice quadrupole structure in these phases is illustrated in Fig. 3. These new 4-sublattice orders $zyzx$ and $zxzy$ also have a finite degeneracy related to the cubic point group, and the degeneracy is 12. Low symmetry of the NS phase questions its stability in better approximations with a larger unit cell, but we leave this issue for a future study.

The full phase diagram is calculated in J - K parameter space and shown in Fig. 2(c). It is quite surprising that the O_{20} AFQ phase is very narrow and destabilized into the $zyzx$ phase, where not only O_{20} but also O_{22} components are nonzero. This comes from a special constraint of the $\Gamma_3 + \Gamma_1$ Hilbert space. Applied by the molecular field $\mathbf{q} = (q_u, 0)$, the response $\langle Q_u \rangle$ grows from $+1$ linearly if $q_u > 0$, but stays -1 if $q_u < 0$. Thus, the O_{20} AFQ phase cannot gain an enough interaction energy, and this is the origin of instability.

We now discuss finite temperature properties of quadrupole orders. At finite temperatures, there appear two new phases which are absent in the ground state: the $zyox$ phase for $K > 0$ and the $zoxxy$ phase for $K < 0$ as shown in Fig. 4(a) for $T=0.5$. The two sublattice structures are shown in Fig. 3, and interestingly they are a partial-ordered phase in which one sublattice remains disordered, i.e., the quadrupole moment vanishes. These two phases emerge through first-order transition as T decreases in a wide region of J - K parameter space. See also Fig. 5, where the J - T phase diagrams for fixed K are shown. We will explain later that they are triple- \mathbf{q} orders of quadrupoles in the fcc lattice.

The other regions in the J - K plane are occupied by the phases discussed for $T=0$: the FQ phase for $J < 0$, the O_{22} AFQ order for $K < 0$ and smaller J , and the $zxzy$ and the NS phases for larger J and $K < 0$. The $zyzx$ phase does not appear at $T=0.5$ in the range shown in Fig. 4(a), but gradually starts to dominate at low temperatures a large region of the $K > 0$ part as shown in Fig. 4(b) and also in Figs. 5(a) and (c). As shown in Figs. 2(c) and 5(c), the O_{20} AFQ phase is limited to a tiny region. This clearly contrasts with the O_{22} AFQ order for $K < 0$. In addition, the O_{20} AFQ phase does not touch the disordered phase (denoted as “para” in Figs. 4 and 5), while the O_{22} AFQ phase does. Indeed, for $K > 0$, a first-order transition generally takes place to the partial-ordered phase $zyox$ at a temperature higher than that the AFQ order sets in. We demonstrate this below.

Since the uniform component of quadrupole moments vanishes in the two triple- \mathbf{q} phase, their analysis is easier than the others. We can write down the Landau free energy in terms of order parameters $\{Q_i\}_{i=1}^3$. They are $\langle Q(\mathbf{k} = \mathbf{q}_i) \rangle$ de-

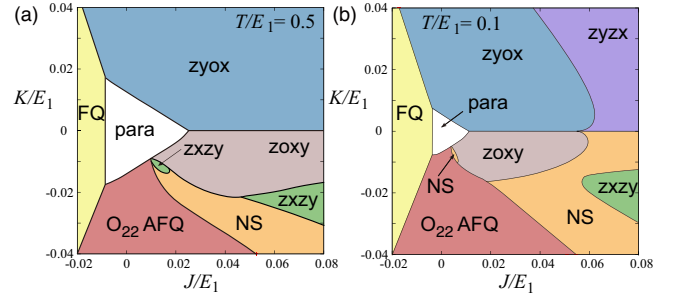


Fig. 4. (color online). J - K phase diagram for $T/E_1 =$ (a) 0.5 and (b) 0.1.

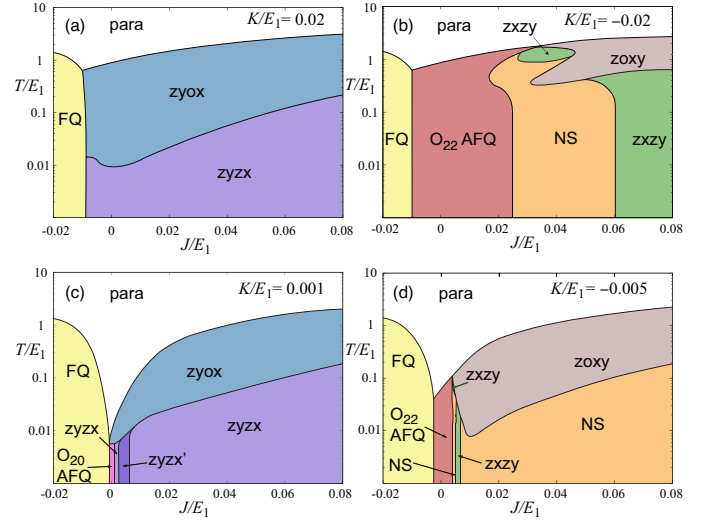


Fig. 5. (color online). J - T phase diagram for $K/E_1 =$ (a) 0.02, (b) -0.02 , (c) 0.001, and (d) -0.005 . “para” denotes the high temperature disordered phase.

finied at the three zone-boundary wavevectors $\mathbf{q}_1 = (2\pi, 0, 0)$, $\mathbf{q}_2 = (0, 2\pi, 0)$, and $\mathbf{q}_3 = (0, 0, 2\pi) = \mathbf{k}_X$, and also parameterized as $\mathbf{Q}_i = (Q_{iu}, Q_{iv}) = Q_i(\cos \theta_i, \sin \theta_i)$ with $Q_i \geq 0$. At these \mathbf{q}_i 's, the exchange interactions $J\gamma_0(\mathbf{k}) + K\gamma(\mathbf{k})$ have the lowest eigenvalue $-2J - 4|K|$ and their eigenvectors correspond to $(\theta_1, \theta_2, \theta_3) = (2\pi/3, 4\pi/3, 0)$ for $K > 0$ and $(7\pi/6, 11\pi/6, \pi/2)$ for $K < 0$. Note that the mode for $\theta_i + \pi$ is equivalent to θ_i , as far as the harmonic parts are concerned. The phase with only one $\mathbf{Q}_i \neq 0$ is a natural choice for discussing the second-order transition of the single- \mathbf{q} order with the highest transition temperature. One can write down the free energy density for general cases as

$$F = \sum_{i=1}^3 \left(\frac{1}{2} a Q_i^2 + c Q_i^4 \right) + 4c' \sum_{i < j} Q_i^2 Q_j^2 \cos^2(\theta_i - \theta_j) - b Q_1 Q_2 Q_3 \cos \bar{\theta} + \dots, \quad (\bar{\theta} \equiv \theta_1 + \theta_2 + \theta_3). \quad (7)$$

Since $\mathbf{q}_1 + \mathbf{q}_2 + \mathbf{q}_3$ is a reciprocal lattice vector, the third-order term is nonvanishing and plays a crucial role in stabilizing the triple- \mathbf{q} phases. Note that one can take $b > 0$ without loss of generality.

For $K > 0$, the triple- \mathbf{q} phase with the choice $(\theta_1, \theta_2, \theta_3) = (2\pi/3, 4\pi/3, 0)$ satisfies $\bar{\theta} = 0$, and thus this gains an energy from the third-order term. This demonstrates that the triple- \mathbf{q} order takes place through a first-order transition with a higher transition temperature than the AFQ order's where $a = 0$. This is a very unique property of the nonmagnetic triple- \mathbf{q} order with \mathbf{q} 's at the Brillouin zone

boundary. Among various possibilities of the triple- q orders, promising candidates are those consisting of the eigen modes with the lowest eigenvalue of $J\gamma_0(\mathbf{k})+K\gamma(\mathbf{k})$. There are two such candidates. One is the triple- q phase with $Q_1=Q_2=Q_3$ and $F=aQ^2/2-2bQ^3/\sqrt{3}+(c+c'/3)Q^4$, where $Q^2\equiv Q_1^2+Q_2^2+Q_3^2$. The other is that with $Q_1=Q_2\neq Q_3=3b/c'$ and $F=aQ^2/2+cQ^4+c'Q_1^4$. While the free energy for O_{20} AFQ is given by $F=aQ^2/2+cQ^4$, one should not compare this directly to those above for the triple- q 's. This is because the optimal value of Q_i 's differs for each phase (the triple- q phases are realized even for $a>0$).

Examining the real-space profile $Q(\mathbf{r})\propto\Re\sum_i e^{i\mathbf{q}_i\cdot\mathbf{r}}Q_i$, it turns out that the former corresponds to the $zyox$ phase which is realized when the moment size is small, while the latter to the $zyzx$ phase when the moment is larger. In Figs. 2(c) and 5(c), a first-order transition occurs inside the $zyzx$ phase with no symmetry change, and we have named the inner-side phase $zyzx'$. The difference lies in the magnitudes of Q_i . At $T=0$, Q_u^C is pinned at -1 in the $zyzx'$ phase, while positive in the nearby region of the $zyzx$ phase. At finite temperatures, $Q_1=Q_2>Q_3$ in $zyzx'$, while $Q_1=Q_2<Q_3$ for $zyzx$. Note that in $zyzx$ and $zyzx'$ phases, the uniform quadrupole moment $\mathbf{Q}_0=\langle\mathbf{Q}(\mathbf{k}=\mathbf{0})\rangle$ is also finite, since another third-order term $-b'\sum_{i=1}^3[Q_{0u}(Q_{iu}^2-Q_{iv}^2)-2Q_{0v}Q_{iu}Q_{iv}]$ gains an energy, while it vanishes in the $zyox$ phase. The direction of \mathbf{Q}_0 is parallel (antiparallel) to \mathbf{Q}_3 in the $zyzx$ ($zyzx'$) phase. When integrating out the uniform component \mathbf{Q}_0 , the form of the free energy is unchanged, but the coefficients c and c' are renormalized.

The part of $K<0$ requires a more elaborate analysis, and we discuss the competition between the O_{22} AFQ and $zoxxy$ phases only qualitatively. In contrast to the case for the $K>0$ part, the triple- q phases consisting of the lowest eigenmode for each of \mathbf{q}_i have no third-order free energy gain, since $-bQ_1Q_2Q_3\cos\bar{\theta}=0$ when substituting $(\theta_1,\theta_2,\theta_3)=(\pi/2,7\pi/6,11\pi/6)$ for $K<0$. Thus, in order to achieve an gain of the third-order term, each \mathbf{Q}_i should be optimized by hybridizing the two eigen modes. We should note that incommensurate orders cannot be ruled out here, but we leave this analysis for a future study.

The simplest triple- q ansatz is a symmetric hybridization with the same amplitude and ‘‘tilting’’ angle ϕ for all the \mathbf{q}_i : $\mathbf{Q}_i=\bar{Q}(\cos(\theta_i-\phi),\sin(\theta_i-\phi))$ with $\theta_i=(4i-1)\pi/6$. This choice corresponds to the $zoxxy$ phase appearing in Fig. 4 for $K<0$. We find its free energy as $F=[a_0/2+4K\cos(2\phi)]\bar{Q}^2+b\sin(3\phi)\bar{Q}^3+\dots$ by approximating $a(K)$ around $K=0$. In contrast, the free energy for O_{22} AFQ with $\mathbf{k}=\mathbf{k}_X$ is $(a_0/2+4K)Q_3^2+\dots$. Thus, the stability of the $zoxxy$ phase is controlled by the cost $4K\cos(2\phi)\bar{Q}^2$ and the gain $b\sin(3\phi)\bar{Q}^3$. For larger $|K|$, as the energy cost increases in the second-order term, the $zoxxy$ phase is not favored, which is consistent with the mean-field results for the microscopic model as shown in Fig. 4.

A crucial stabilization mechanism of the triple- q phases such as $zyox$, $zyzx$, and $zoxxy$ discussed above is the third-order invariant in the free energy. This differs strikingly from magnetic systems, where it is prohibited by the time-reversal symmetry. Within the Landau theory, the mechanism stabilizing the other phases depends on the details of the higher-order terms and the coupling with the uniform quadrupole moment \mathbf{Q}_0 in the third- and fourth-order terms.

In this paper, we have theoretically studied electric

quadrupole orders of non-Kramers local doublets Γ_3 states on the fcc lattice. To this end, we constructed a minimal effective model by taking account of the lattice structure, and analyzed it by a four-site mean-field theory. Its Hamiltonian has three energy scales: isotropic and anisotropic exchange constants J , K , and the excitation energy of the Γ_1 state E_1 . It has been known that the ratio $\sqrt{J^2+K^2}/E_1$ measures the strength of the Z_3 anisotropy characteristic to systems with time-reversal symmetry such as electric quadrupoles. The limit of negligible Z_3 anisotropy ($\sqrt{J^2+K^2}/E_1=0$) has three ordered phases: ferro, and two 2-sublattice antiferro phases (O_{20} - and O_{22} -antiferro).

When the excitation energy E_1 is not so large, the Z_3 anisotropy produces considerable effects and stabilizes phases with more complex quadrupole structure. Two of them are the $zyox$ and $zoxxy$ phases, and they have 4-sublattice antiferro partial orders that quadrupole moment is zero in one sublattice. These two are also special in that the ferro component of quadrupoles vanishes, while the other 2- and 4-sublattice antiferro phases have a nonzero parasitic ferro component. One can understand that these partial ordered phases are a triple- q order that the Z_3 anisotropy couples the three modes with wavevectors $(2\pi, 0, 0)$, $(0, 2\pi, 0)$, and $(0, 0, 2\pi)$. The results of our calculations propose quite many candidates for the discussed quadrupole antiferro order that takes place in the material PrMgNi_4 . A first screening would be the checking whether the cubic lattice symmetry is broken or not, and its result narrows the order identification. The direction of the order parameter $\langle\mathbf{Q}(\mathbf{r})\rangle$ determines the lowered local symmetry at each Pr ion, and probing atomic displacements also helps in identifying the order.

Acknowledgment This work was supported by a Grant-in-Aid for Scientific Research (Grant Nos. 16H04017 and 18K03522) from the Japan Society for the Promotion of Science.

- 1) K. Hattori and H. Tsunetsugu, J. Phys. Soc. Jpn. **83**, 034709 (2014).
- 2) K. Hattori and H. Tsunetsugu, J. Phys. Soc. Jpn. **85**, 094001 (2016).
- 3) T. Ishitobi and K. Hattori, J. Phys. Soc. Jpn. **88**, 063708 (2019).
- 4) T. Onimaru and H. Kusunose, J. Phys. Soc. Jpn. **85**, 082002 (2016).
- 5) A. Sakai, K. Kuga, and S. Nakatsuji, J. Phys. Soc. Jpn. **81**, 083702 (2012).
- 6) T. Taniguchi, K. Hattori, M. Yoshida, H. Takeda, S. Nakamura, T. Sakakibara, M. Tsujimoto, A. Sakai, Y. Matsumoto, S. Nakatsuji, and M. Takigawa, J. Phys. Soc. Jpn. **88**, 084707 (2019).
- 7) S. Kittaka, T. Taniguchi, K. Hattori, S. Nakamura, T. Sakakibara, M. Takigawa, M. Tsujimoto, A. Sakai, Y. Matsumoto, and S. Nakatsuji, J. Phys. Soc. Jpn. **89**, 043701 (2020).
- 8) T. Onimaru, K. T. Matsumoto, Y. F. Inoue, K. Umeo, T. Sakakibara, Y. Karaki, M. Kubota, and T. Takabatake, Phys. Rev. Lett. **106**, 177001 (2011).
- 9) K. Iwasa, K. T. Matsumoto, T. Onimaru, T. Takabatake, J.-M. Mignot, and A. Gukasov, Phys. Rev. B **95**, 155106 (2017).
- 10) T. Onimaru, T. Sakakibara, N. Aso, H. Yoshizawa, H. S. Suzuki, and T. Takeuchi Phys. Rev. Lett. **94**, 197201 (2005).
- 11) Y. Sato, H. Morodomi, K. Ienaga, Y. Inagaki, T. Kawae, H. S. Suzuki, and T. Onimaru, J. Phys. Soc. Jpn. **79**, 093708 (2010).
- 12) R. Shiina, H. Shiba, and O. Sakai, J. Phys. Soc. Jpn. **68**, 2105 (1999).
- 13) Y. Kusanose, T. Onimaru, G.-B. Park, Y. Yamane, K. Umeo, T. Takabatake, N. Kawata, and T. Mizuta, J. Phys. Soc. Jpn. **88**, 083703 (2019).
- 14) Y. Kusanose, T. Onimaru, G.-B. Park, Y. Yamane, K. Umeo, and T. Takabatake, JPS Conf. Proc. **30**, 011160 (2020).
- 15) S. B. Lee, S. Trebst, Y. B. Kim, and A. Paramekanti, Phys. Rev. B **98**, 134447 (2018).
- 16) F. Freyer, J. Attig, S. B. Lee, A. Paramekanti, S. Trebst, and Y. B. Kim, Phys. Rev. B **97**, 115111 (2018).

- 17) F. Freyer, S. B. Lee, Y. B. Kim, S. Trebst, and A. Paramekanti, Phys. Rev. Reserach **2**, 033176 (2020). S. Nakatsuji, and Y. B. Kim, Nature Comm. **10**, 4092 (2019).
- 18) K. Kubo and T. Hotta, Phys. Rev B **95**, 054425 (2017).